Concepts and Modelling in Geomorphology: International Perspectives,
Eds. I. S. Evans, R. Dikau, E. Tokunaga, H. Ohmori and M. Hirano, pp. 61–84.

Scale-Specific Landforms and Aspects of the Land Surface

Ian S. EVANS

Earth Surface Systems Research Group, University of Durham, England;
Department of Geography, Science Laboratories,
South Road, Durham, England DH1 3LE, U.K.
e-mail: i.s.evans@durham.ac.uk

Abstract. The land surfaces of Earth, of other planets and of moons show both scale-specific and scaling behaviour. Size and spacing of landforms often show clustering around characteristic scales or between limits related to process thresholds or to the space available. This is clearest for various bedforms, in dynamic equilibrium with the last dominant flow or several flows. It is also clear for glacial cirques and for some types of landslides, sinkholes, abyssal hills and volcanoes.

Strong scale-specificity as in cirques may be global. Weaker forms of scale specificity are also recognised, limited by either material or process variations to regions or to locales. The implications of global, regional and local scale-specificity are explored. Even the weaker forms of scale-specificity are not expected on surfaces generated by fractal models.

The contrast between efficiency of surface flow and of consistently channelled flow imposes a lower characteristic scale (length of slope, drainage density) on fluvial erosional topography. The most common horizontal scales observed in the Earth's topography are (1) tens or hundreds of m for slopes to (minor) streams; (2) km for major slopes, relevant to deep bedrock landsliding; and (3) tens to hundreds of km for broader tectonic and volcanic relief features. The internal properties of the Earth's lithosphere and mantle impose limits to relief.

Scaling may involve statistical self-similarity or self-affinity (fractal behaviour) over a few orders of magnitude, but is bounded by both upper and lower limits. Scaling is also found, over more limited ranges, for the characteristics of scale-specific features such as cirques and dunes. Scaling may be isometric (constant shape) or allometric (shape changes with size). Clear thresholds in the impact cratering process give changes in morphology and breaks of slope in depth: diameter scaling plots; these vary in orderly fashion between different planets and moons. Given the number of scale thresholds evident in geomorphology, it is dangerous to use scaling relationships for extrapolation beyond the data on which they are based.

Keywords: Fractal, Scaling, Relief, Bedforms, Landslides, Cirques, Craters

INTRODUCTION

The scale-specific nature of the land surface cannot be denied: nor can the scaling relationships between geometric attributes over certain ranges. Wherever landforms can be defined, there is an upper and a lower limit to their size. At the least the upper limit is less than the whole Earth and the lower limit is greater than

sedimentary grain size. Taken globally, features such as river channels, landslides, alluvial fans and volcanic cones cover broad ranges of size, but others such as cirques, drumlins and dolines cover narrower ranges, typically one decimal order of linear magnitude—a factor of 10 difference between the widest and the narrowest. The geomorphometry of specific landforms often demonstrates specific scales, especially for equilibrium forms (mainly bedforms). Non-equilibrium forms, by definition growing or decaying, are likely to cover broader size ranges, but they too are limited by thresholds.

Most landform sizes and spacings show large numbers of small values and smaller numbers of large ones. Thus it is natural to view them on logarithmic scales, and to consider their log-normality—their fit to the log-Gaussian probability distribution. Among the many right-skewed unimodal models for frequency distributions, the main simple alternatives to the log-normal are the exponential and Pareto (power function) distributions, where the most frequent values are at the lowest magnitude. The distribution at middle to high values may differ little between the three models: thus large data sets are needed to provide discrimination, but these are infrequent even today. Johnson *et al.* (1994) provided comprehensive information on all the distribution models considered here: Cox (1992) discussed the use of probability plots in choosing between right-skewed distributions (specifically the exponential and gamma). What is most crucial in distinguishing the log-normal is the existence of a left-hand declining limb, so that on a log scale of magnitude the smaller values are of declining frequency. Testing this requires careful consideration of completeness of inclusion of smaller values, since a phased truncation or censoring of the data might create a spurious declining limb.

It may be misleading to consider the global distribution of sizes. Although cirques are globally scale-specific, there are other landforms which are scale-specific in a given region or locality. Lineation and streamlining are usually associated with scale-specificity. Landforms such as yardangs (streamlined forms eroded by the wind) are locally similar in size, but vary tremendously between areas, mainly because they are eroded into different materials over different time-spans.

Scale-specificity involves not only size frequency distributions, but also breaks in slope in power and other plots which otherwise exhibit fractal-like scaling. Such breaks relate to process thresholds, whereas size limits may reflect either thresholds or constraints on the space available. When a threshold is crossed a new feature emerges, such as a slip face in a pile of aeolian sand, or a central peak in an impact crater. Such thresholds limit positive feedbacks (from form to process and back) that would produce runaway, scale-free forms. Negative feedbacks, on the other hand, directly provide limits to the scale of landforms. Thus scale-specificity is found in both exogenetic and endogenetic process—form relationships, and on both moons and planets.

Landform scale-specificity and scale-dependency is recognised by geomorphologists either implicitly or explicitly (Evans, 1972; Wood, 1996; Wilson and Gallant, 2000, p. 31). One may wonder at the necessity for a review

such as this; but many other scientists and engineers are now concerned with the land surface as represented in Digital Elevation Models and find scale-free fractal models a seductive approach. Hence there is a need to be explicit, to compile and to analyse hard evidence for scale-specificity. Here we first consider scale-specificity in bedforms (aeolian, fluvial and glacial), then in some specific erosional forms (glacial cirques, karst sinkholes, landslides and fluvial slopes) and finally in tectonism, isostasy, volcanoes and meteorite impact craters. It is not possible to be comprehensive, but consideration of contrasting process-systems provides revealing comparisons. Specific scales are shown to be related to thresholds or to space constraints.

AEOLIAN BEDFORMS

Both yardangs and dunes are aeolian bedforms, formed by the interaction of a fluid current with erodible and transportable land surface material. Mini-yardangs, of centimetric scale, form rapidly on sandy beaches as initially wet sand dries and is eroded by moderate wind. Yardangs form over centuries when lake sediments dry out and are eroded by unidirectional winds: those in Egyptian lake sediments at Kharga are 0.5 to 8.7 m high (Goudie, 1999). In the Holocene diatomites of Chad, their crests are spaced (transverse wavelength) 20 to 50 m apart (Mainguet, 1972, plates LXXIV and LXXVI). Nearby crests and corridors in Palaeozoic sandstone have a 1.6 km spacing and can be considered as long mega-yardangs: illustrations in Hagedorn (1971, Abb. 74–82) show that the long ridges grade into shorter yardangs and are sometimes oblique to structure. The landscape is dominantly aeolian and implies that the Northeast Trades have been stronger and persistent through much of the Quaternary, amplified by deflection around the Tibesti massif. The lake sediments with yardangs penetrate the corridors between the mega-yardangs (Mainguet, 1972), but there are no intermediate features. Yardangs are not found on the backs of the larger features, and they do not have mini-yardangs on their sides or tops: the microrelief is quite different from the broader form (Whitney, 1983). Apart from the relation to material erodibility, it is hard to explain the variation in yardang size, and its regional regularity. Yardangs are found even in resistant granites and marbles in Egypt.

Mini-yardangs are superimposed on beaches that are smooth for hundreds of metres. Thus none of these landscapes can be described as self-similar or fractal: they are ordered, and their scale is clear. The yardang family as a whole is not globally scale-specific except in its upper size limit: it is, however, locally or regionally scale-specific. It can also be found on other planets. Greeley and Iversen (1985, pp. 143–144) illustrate some very regular lineations in the equatorial regions of Mars, which are likely to be due to wind erosion. Their transverse spacing is 2 km in the western Tharsis region (about 92 ridges in 181 km) and 280 m in the Aeolis region (46 in 13 km).

Among aeolian landforms, the regularity of sand dunes is well known (Cooke *et al.*, 1993), although size and spacing do vary regionally and some

'hierarchies' are recognised. At the edge of a dune field, the change in surface properties is abrupt. Sand dunes are often superimposed at two different scales. In a given region, however, both dunes and megadunes (draa) of a particular type vary little in height and spacing (Lancaster, 1988). Where dunes are superimposed on draa, there is an order of magnitude difference in scale between the two (Lancaster, 1988, figure 2). There is a clear gap in size and spacing between the two types, and some qualitative differences between dunes and draa, so the relationship is not gradational. Both the dunes and the draa are regionally scale-specific, each covering half an order of magnitude or less. The contrast between them is strongest in the time taken to move one wavelength: this is three orders of magnitude greater for Namib draa than for their superimposed dunes.

Desert dunes are spaced hundreds of metres apart, up to several km. Considering transverse and longitudinal dues in the northern Sahara, Wilson (1971, 1972) distinguished dunes, with wavelengths of 3 to 100 m, from draa (megadunes) with wavelengths of 300–5500 m. He maintained (1972, p. 185) that ripples, dunes and draa are distinct, and do not grow or shrink into one of the other two. For each, the greater wavelengths are in coarser sand, so that for a given material the ranges of wavelengths are well under one order of magnitude. Apparently this relationship is regional: later workers such as Wasson and Hyde (1983a, b) and Lancaster (1988) did not find a general relation between dune spacing and grain size in Australia or southern Africa.

Within ten different regions and dune types, spacing varies less than an order of magnitude (Lancaster, 1988, figure 1). Simple barchan dunes are mainly 1–12 m high and 25–100 m wide: or, according to Allen (1982, vol. 1, p. 320), "Most barchans have a height of 2–20 m and are usually homogeneous in scale within any one area." Not only are they scale-specific, but also within their limited size range their shape changes systematically with size. A slip face is formed when a dune reaches a threshold height, of the order of a metre. In larger barchans, the slip face and the horns become relatively more important (Sauerman *et al.*, 2000).

A full survey of Australia's desert dunes, which are mainly linear and without draa, shows a mean transverse spacing of 560 m (mode 270 m) (Wasson *et al.*, 1988, figure 10). The cores of most dune-fields show spacings less than 300 m. Greater spacings are most common on coarser sands, toward the periphery of dune-fields.

Star dunes are among the highest: in some regions they show two clear scales, an order of magnitude apart. In the Namib Desert, their heights are unimodal and mainly 50–200 m; widths are 400–1000 m and spacings 600 to 1800 m, averaging 1330 m. Comparative figures for a range of studies on different continents, by different authors, are height mainly 50–350 m, width 200–3000 m, and spacing 160–4000 m (Lancaster, 1989). Thus star dunes are scale-specific, especially regionally. They develop under multidirectional winds, with abundant sand supply but little net movement: seasonal variations in sand flow cancel out.

Dunes in general are at least regionally scale-specific in their dimensions and spacings. The lower size limit reflects the ease with which small sand patches are dissipated. Upper limits to height may reflect exposure to greater wind forces.

GLACIAL AND FLUVIAL BEDFORMS

Currents in water and in ice also produce bedforms, which tend to be lineated or streamlined as well as scale-specific. Fluvial and marine dunes, antidunes and sand waves cover at least two orders of magnitude, but their dimensions increase with depth of current (Allen, 1982 vol. 1, pp. 331–334, 410 and 456) and are thus locally scale-specific.

Drumlins and flutings form beneath glaciers, and sand ribbons and sand waves form on continental shelves. Drumlins have regionally consistent spacings, heights and widths, although lengths are more variable. Mean widths in 17 drumlin fields studied by Mills (1987) in the USA were between 110 and 437 m (mainly 200 to 360 m): studies in Europe extend this range of means to 128 to 755 m. Mean height varied only from 6 to 24 m in the USA study, but from 4 to 52 m in European studies. For individual drumlins, the overall width ranges over one order of magnitude; drumlins can be regarded as globally scale-specific. There are trends in size and shape within drumlin fields, so that locally drumlins are highly scale-specific. In some areas, drumlins merge into more elongate fluting forms: in Alberta, these have transverse wavelengths around 100 or 200 m (Gravenor and Meneley, 1958) whether in bedrock, till or water-laid sediments.

At a different scale, the flutings observed on many glacier forelands show striking regularity as well as parallelism. For example, those in front of one Norwegian glacier are around 0.3 m high (range 0.07 to 1.13) and 3 m wide (range 0.5 to 9.7) (Gordon *et al.*, 1992, pp. 717–718). These are unlikely to show transitions to drumlins or the related large flutes. They may relate to deforming debris-rich basal ice, rather than to deforming sediments.

Bedforms of mobile material, such as dunes and many drumlins, are limited in size either by the negative feedback of stronger currents at the crests of higher forms, or by instabilities tending to split them more often than merging them.

GLACIAL CIRQUES

A different category includes erosional features such as landslides, dolines and glacial cirques, none of which are bedforms. Evans and McClean (1995) demonstrated scale-specificity in glacial cirques, and their evidence is extended in Table 1 to four large data sets. Cirque lengths and widths approximate Gaussian distributions on the logarithmic scales that are appropriate to most size measurements. The reduction of skewness to near zero confirms the appropriateness of the logarithmic scale, and the similarity of median and geometric mean confirms symmetry on that scale. The consistently low standard deviations (SD) demonstrate strong regional scale-specificity; the range within each region is only one order of magnitude. Means vary little, supporting the concept of cirques as globally scale-specific. Evans and McClean (1995, table 1) gave logarithmic (base 10) standard deviations, all of them low, for further size measures, six in all.

The minimum size is related to thresholds for glacier formation: the maximum, to available space on slopes or at valley heads. Width across a valley head is more obviously limited than length downvalley, yet both width and length of cirques

Table 1. Length and width of Glacial Cirques. The geometric mean, the antilog of the mean on the logarithmic scale, is the most appropriate measure of central tendency for frequencies that are log-normally distributed.

Range	*N*	$\log_{10}$ *scale*		*median*	*geometric*	*skewness:*	
		mean	*SD*		*mean*	*initial*	$\log_{10}$ *scale*
CIRQUE LENGTH :							
Bendor , B.C.	186	2.87	0.186	735 m	741 m	1.42	0.10
Cayoosh, B.C.	198	2.85	0.206	670 m	708 m	1.67	0.04
Wales (provisional)	228	2.80	0.192	620 m	631 m	2.03	0.29
Lake D., England	158	2.75	0.190	535 m	562 m	1.36	0.18
CIRQUE WIDTH :							
Cayoosh, B.C.	198	2.82	0.215	625 m	658 m	1.79	0.42
Wales (provisional)	228	2.84	0.181	686 m	656 m	1.41	0.19
Lake D., England	158	2.79	0.187	600 m	621 m	0.85	-0.02

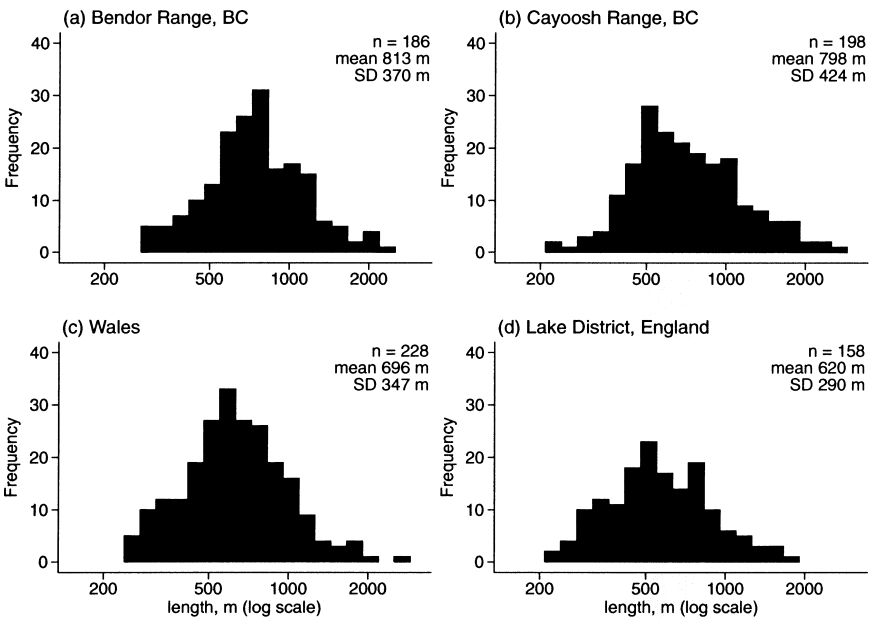

Fig. 1. Logarithmic histograms of cirque lengths in British Columbia and in Britain: (a) Bendor range, B.C.; (b) Cayoosh Range, B.C.; (c) Wales; and (d) the Lake District, England. Note the symmetry between left and right limbs, not suggesting truncation.

are scale-specific. Histograms of cirque length (Fig. 1) on a logarithmic scale show clear declining limbs on both upper and lower sides. Quantile-quantile plots (e.g. Evans and McClean, 1995, figure 2) confirm the excellent fit of log-normal distributions to length, width and wall height for all four sets of cirques in Table 1. De Blasio (2002) shows that this size distribution can be modelled by stipulating that much of the surface is unsuitable for cirque development: otherwise (on his assumption, of growth from small hollows) there would be a proportion of small, recently formed cirques. I prefer the interpretation that snow-patches are not effective erosion agents (Evans, 1997), and cirque development only starts when threshold thickness and horizontal dimensions permit development of a glacier, with significant basal movement.

Within their specific range of scales, cirques do show power-function relations, for example between vertical and horizontal dimensions (Evans and McClean, 1995) there is allometry (change in shape with size: Church and Mark, 1980). Scaling may thus be complementary, not contradictory, to scale-specificity.

KARST

Unlike depressions in fractal surfaces, karst depressions do not give size and shape distributions that mirror those of elevations. Sinkholes or dolines are the most common type of karst depression, and they are produced by solution of limestone, gypsum or sodium chloride, often followed by subsidence of overlying rocks. Sinkhole depths (Troester *et al*., 1984) and diameters (White and White, 1987) approximate exponential frequency distributions. Log-log plots are decidedly non-linear: sinkhole populations are not fractal. On carbonate in Kentucky, a typical width is around 200 m: on gypsum in Uzbekistan, depressions are tightly clustered around a width of 10 m. The 2800 dolines plotted by Gorbunova (in Klimchouk and Andrejchuk, 1996) cover two orders of magnitude, but are developed on a range of cover rock thicknesses.

Karst towers in northern Puerto Rico range in height from 5 to 52 m. For 149 measured by Day (1978), the modal height is 12 m, the median 16 m and the mean 19 m: the standard deviation is 10.7 m. The frequency distribution (Day, 1978, figures 3 and 4) seems close to log-normal.

On a narrower scale, the width and length of clints on limestone pavements, and the depth and width of the grikes separating them, are log-normally distributed with limited variation (Goldie and Cox, 2000). This is an example of characteristic scales in rock structure producing similar scales in the land surface. Solution flutes (Rillenkarren) on limestone show limited variation in each area: for example, those measured by Mottershead (1996) in Majorca average 17 mm wide, with a standard deviation of only 3.2 mm for the means of 30 sets of flutes.

LANDSLIDES

Landslides are a very broad category and range over about 4 orders of linear magnitude globally (metres to tens of kilometres: note that two orders of area equate to one order of length). However, in a particular region a specific type of

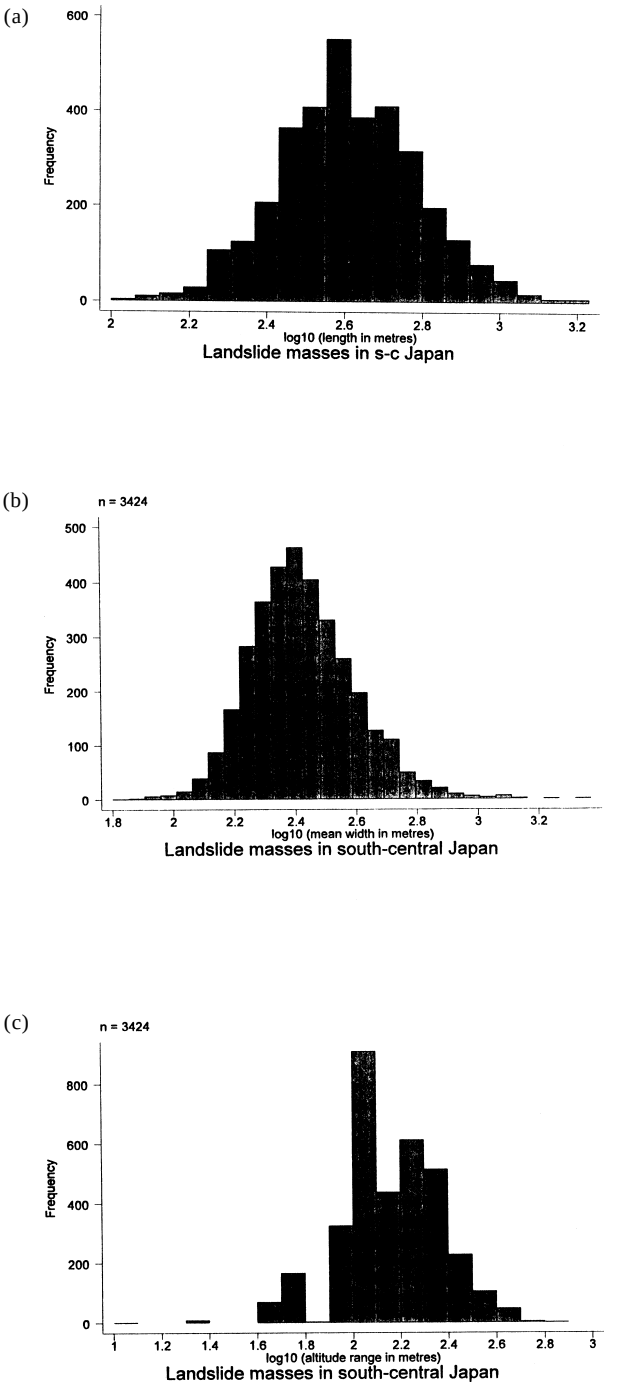

Fig. 2. Logarithmic histograms of (a) length; (b) mean width and (c) altitude range of 3424 landslide masses in south-central Japan (data supplied by Sugai and Ohmori).

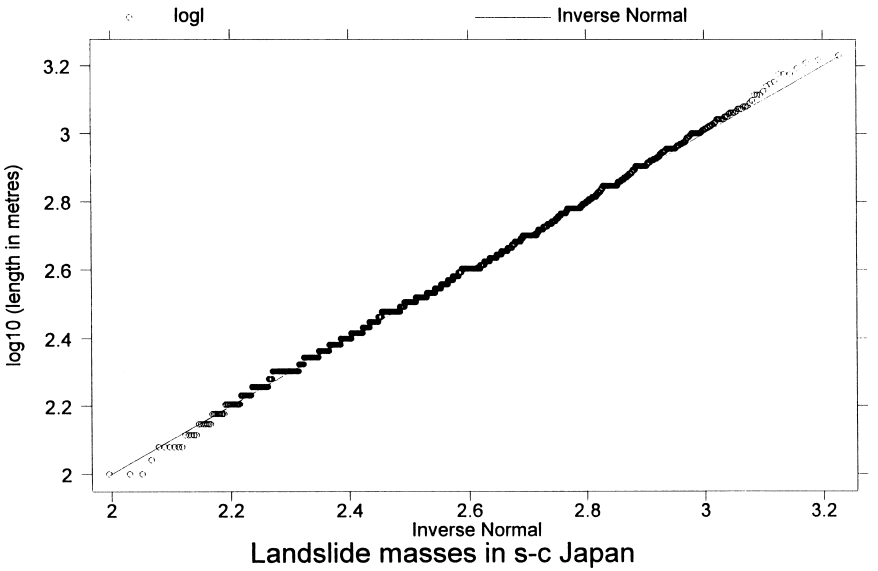

Fig. 3. Logarithmic quantile-quantile plot of landslide mass length in south-central Japan (data supplied by Sugai and Ohmori). The quantiles are the data ordered by magnitude. Each quantile is plotted against the corresponding quantile of the Gaussian frequency distribution with the same mean, standard deviation and sample size. Linearity shows the excellent match of this large data set to the log-normal frequency distribution.

landslide may have a characteristic scale, depending mainly on material properties and slope form. Testing this concept requires large data sets based on regional inventories. One of these covers 3424 landslide masses in the Akaishi Range, south-central Japan (Sugai *et al*., 1994). As for most landforms, the size distribution is positively skewed: the mode and median length are 400 m and the mean is 446 m. There is some rounding to a 50 m interval. Logarithmic transformation provides an excellent symmetrical distribution (Fig. 2), tightly clustered around the geometric mean of 409 m, 2.61 on the scale $\log_{10}$ (metres). On the same scale the standard deviation is 0.18, very similar to the cirques of Table 1. For mean width, defined as area/length, the standard deviation is 0.17 and for range in altitude of the landslide mass (excluding the scar) it is 0.21 (Fig. 2). The quantile-quantile plot (Fig. 3) shows how closely the data fit the log-normal distribution.

In fact the landslide masses are at a broad range of altitudes, and on 11 different geological formations for which mean lengths vary from 387 to 505 m (Ohmori and Sugai, 1995, table 1): for these more tightly defined groups, standard deviations are less. These authors stated that they "tried not to miss any of the masses larger than 10,000 m^2" (Ohmori and Sugai, 1995, p. 153): "landslide masses smaller than 10,000 m^2 were not counted" (Sugai *et al*., 1994, p. 237), corresponding to a linear dimension of about 100 m. It is safer to assume that coverage is near-complete for masses over 200 m long, and on this basis I

infer that the decline in frequency below a length of 400 m is not an artefact due to under-sampling. Hence these landslide masses in the Japanese Alps are regionally scale-specific.

Stark and Hovius (2001) come to different conclusions for landslides in mountainous parts of New Zealand and Taiwan. Their size range from 100 to 300,000 m^2, corresponding to 10 to 550 m linearly, is rather less than two orders of magnitude. Modal frequency on a logarithmic scale is around 1000 m^2 in each case, suggesting a dominance of smaller landslides than in Japan. Stark and Hovius (2001) suggest that the decline in frequency for smaller landslides results from under-sampling, which seems more likely for their linear dimensions below 30 m than for those below 400 m in Japan. They fit power functions to the right-hand limbs of the frequency distributions, but admit (p. 1081) that the power law fit is adequate only for part of the distribution with 25% of the observations. They are able to simulate observed distributions on the assumption that landslides are under-sampled according to a positive quasi-power-law relationship, below apparent mapping resolutions of 28 m and 42 m for two air-photo-based studies in New Zealand. To confirm that under-sampling occurs in this way requires a very detailed field study.

Montgomery *et al*. (1998) mapped 3224 shallow landslides in western Washington and Oregon, mainly between 20 and 220 m across. They found a roughly exponential distribution of landslide areas, with a median of 3386 m^2 and a mean of 8152 m^2. The general conclusion that landslides follow power-law scaling for all size ranges ("scale invariance is a general property of the landslide mechanism"; Hovius, 2000, p. 83) may be premature. It is likely that more precisely defined landslide types follow log-normal or exponential distribution models. Their lower size limits are thresholds specific to the type. Their upper size limits (a length of 1 km in New Zealand; Hovius, 2000) are controlled by slope height and length, characteristics of the topography in a particular region. Each landslide type is regionally scale-specific, even though landslides globally cover a wide range of scales and exhibit scaling behaviour over limited ranges. Recognition of this may require classification of types, at the level of rotational slumps, debris flows and rock avalanches: the category 'landslide' may be too broad. If too diverse a group are pooled, some essential scale-specific aspect may be lost, e.g. the transition from simple to complex landslides, or single movements to multiple movements.

FLUVIAL SLOPES

Some aspects of the land surface appear similar in form when viewed at different scales—notably the dendritic drainage channel networks found in many regions. However, these are not scale-free because the initiation of a channel requires runoff from a threshold area: this varies as a function of rainfall, slope gradient and soil properties. Measurement of channel density necessarily implies mean spacing and thus scale-specificity. Tarboton *et al*. (1992) defined this basic length scale of the (fluvial) landscape as the point where domination by stable diffusive processes (such as creep) gives way to unstable channel-forming

processes. Dietrich *et al*. (1993) considered thresholds of slope stability and of saturation, but found that the main threshold for channel initiation is in the critical shear stress of erosion by overland flow. The critical support area to generate a channel declines with increasing local valley slope (Montgomery and Dietrich, 1992), over a length range from about 30 to 300 m in coastal California and Oregon. Thus for each region there is a characteristic horizontal scale related to channel initiation; channel density is a useful concept even though the network of flow expands and contracts in response to weather events. There are various ways of measuring this characteristic horizontal dimension (reviewed in Evans, 1972, pp. 33–36) and it is not easy to agree on a single figure.

Channel initiation depends on resistance and gradient as well as discharge, so there is considerable inter-regional variation in this scale-specificity. For example, Vandekerckhove *et al*. (2000) found the threshold drainage area for gully initiation in Iberia and Greece to vary between the squares of 6 m and 200 m. The area was less on steeper slopes and varied also with vegetation, land use history and antecedent moisture. One complication pointed out by Dietrich and Montgomery (1998, p. 40) is that the fundamental hillslope for deep landsliding is much bigger than that for fluvial processes.

Furthermore, in some regions with steep slopes, landsliding limits the height and gradient of slope which can be supported, giving a distinctive scale to valley-side relief. Thus stream heads, valley spacing, slope height and gradient are regionally scale-specific features. Gullies on lateral moraines form within clear geometric constraints. These constraints cause regularity in length, in width and thus in spacing (Blair, 1994, figure 9). This local scale-specificity is further maintained by slope collapse if moraine height exceeds a threshold, between 120 and 132 m for the Tasman Glacier (Blair, 1994). Further processes that can produce impressively regular grooves include tephra avalanches, passing radially down the slopes of volcanoes. Allen (1982, vol. 2, p. 420, after Richards) illustrated a large and very regular set, 1–3 m deep and 3–7 m wide, on the upper flanks of Bárcena Volcano in Mexico. Alluvial fans have a wide range of areas (over four orders, or two linear orders), but within a region their length, width and vertical range each vary over one to two linear orders (Blair and McPherson, 1994).

Hovius (1996) demonstrated regular spacing of the main streams (those rising near the main divide) in ten different mountain ranges. Spacing at the mountain front (the Himalaya are an exception) averages just over twice the distance between the front and the main divide. For seven ranges, spacing varies essentially between 3 and 35 km.

For several areas in southern France, Vergne and Souriau (1994) found lineation of detrended topography at scales greater than 2 or 3 km, related to lineation of the main drainage. At shorter scales the topography tends to isotropy and a fractal interpretation may be considered. In the mountains of central Japan, Oguchi (1997) found that total drainage density varied only between 8 and 13 km km^{-2} over a range of igneous, volcanic and sedimentary rock types with relief (in 500 m squares) of 50–550 m. Standard deviations within each type were low, 1.2

to 3.3 km km^{-2}. He related this to uniform spacing of ridges, i.e. 'grain'.

The classic geomorphic concept of 'grain' was defined by Pike *et al*. (1989, p. 129) as "the characteristic horizontal spacing of major rivers and valleys", and shown by them to be equivalent to the concept of 'range' in geostatistics. Either range or standard deviation of altitude is plotted against circle diameter or area, and it is assumed that a single point is reached where the increase (in relief) flattens out. This diameter should be the length of major slopes, and can be used to define a characteristic vertical dimension, relief over a natural rather than an arbitrary area. Note that fractal surfaces will not give such a break point.

With real data, convex plots or multiple break points are often found, but the resulting subjectivity can be reduced by fitting all possible pairs of regression lines (starting from high and from low values) and taking the intersection of the pair that minimise root mean square deviations (Pike *et al*., 1989). This gave 'grain' (valley spacing) values of 1 to 3 km for the Montara Mountain area of San Mateo County, California. Previous manual studies showed grain varying from 2 to 13 km in southern New England, New York and Georgia, USA and from 3 to 24 km in central Europe, but from 3 to 48 km in the Alps. The latter surely exceeds the fundamental hillslope length even for deep landsliding. Such long grain distances may reflect the 3-D nature of glacially-modified valley networks, and broader tectonic forms. The initially 2-D concept of grain needs to be replaced by the expectation of multiple breaks in plots of relief v. diameter—and in variograms.

Dietrich and Montgomery (1998) recognised four specific scales in the fluvial landscape: the channel head, as discussed above in relation to drainage density; channel width and meander wavelength, not discussed here; the change from straight channel slopes to concave-up ones, reflecting a change in the ratio between classic process coefficients m and n (at a drainage area of some 0.8 km^2 in their figure 2.6 for north-western California—i.e. major slopes or valley-sides); and erosional unloading producing isostatic compensation at wavelengths from 100 to 1,000 km because of crustal rigidity (see below). They consider that drainage density sets (minor) hillslope length, which in turn influences hillslope height (local relief). I suggest, however, that relief and grain relate to their third scale rather than their first.

Attempts to fit scale-free fractal models to the land surface have instead established further scale-specific features. Fractal dimensions estimated at broad scales (around 200 km) are about 2.66, considerably higher (rougher surfaces) than those of 2.1 to 2.4 obtained at the erosional landscape scale (around 200 m) (McClean and Evans, 2000). Mark and Aronson (1984) found convex-up scale breaks at 330 to 1800 m, in variograms for mountainous parts of the USA at separations from 150 m to 5 km. I interpret the breaks as lengths of characteristic slopes, the topographic 'grain' beyond which altitude variance increases little: i.e. they are half the major ridge spacing. Estimated fractal dimensions over shorter separations averaged 2.2, while those above the scale break exceeded 2.5. At broader scales, for variogram analyses of large islands with generally high apparent fractal dimensions, McClean and Evans (2000, table 3) observed two

scale breaks, at 8–54 km and at 75–290 km. For continents, Australia and South America show breaks around 100 km (but North America does not). These breaks may relate to broad-scale relief, limited by isostasy and tectonism.

TECTONIC AND RELIEF

Tectonic and isostatic processes are responsible for broader specific scales in topography. The 5 km mean altitude of the Tibetan Plateau may be the highest supportable by current tectonic stresses balanced against lateral spreading in the asthenosphere (Bird, 1991): potential energy increases as the square of altitude, imposing a vertical scale limit. The flexural rigidity of the Earth's crust spreads isostatic depression due to loads of volcanoes over distances such as 200 km for Hawaii. The wavelength varies with the load and with effective elastic thickness of the crust, which varies between 4 and 130 km in North America as lithospheric thickness and temperature vary (Bechtel *et al*., 1990). Thus wavelengths of displacement vary both within and between oceans and continents, providing at best regional scale specificity.

The relief (vertical range or dispersion of altitude) in any region has an upper limit, due to the interaction between uplift, erosional processes and rock strengths. Globally, the subaerial maximum range is in the Himalaya, about 6,500 m around Nanga Parbat and Dhaulagiri. From variogram analyses (reflecting considerable averaging), the standard deviation of altitude differences increases to a maximum (in Asia) of about 1,900 m, at separations in excess of 1,200 km (McClean and Evans, 2000, p. 376).

Brozovic *et al*. (1997) note that in the northwestern Himalaya mean altitude varies with snowline (ELA). They infer that glaciation and frost action above the snowline are faster than fluvial erosion below (Hallet *et al*., 1996; Evans, 1997): only a small proportion of the topography can exceed altitudes 2 km above ELA. In such high relief areas, slopes (above streams or glaciers) have reached limiting gradients and heights maintained by landsliding (Schmidt and Montgomery, 1995; Burbank *et al*., 1996).

VOLCANIC

Globally, volcanoes cover a wide size range, but more specifically, continental stratovolcanoes (cones composed of both lava and ash) are several km across and mainly 500 to 3000 m high (above their bases); a chain of 46 in the central Andes (de Silva and Francis, 1991) are spaced on average 30 km apart. Francis and Abbott (1973) plotted height above base for all 181 continental conical composite volcanoes and found a clear mode around 1750 m (Table 2). They suggested that caldera formation, and possibly a limit to the sustainable height of a magma column, make it difficult for volcanoes on land to exceed a relative height of 3500 m. Parasitic cones, of which there may be dozens on a stratovolcano and more on a shield volcano, have a distinct scale of hundreds of metres. Scales vary between planets: the main volcanic centres on Mars and Venus are hundreds of km across. For young oceanic (hot spot) volcanoes on Earth, Vogt (1974b) found that height

Table 2. Relative heights of volcanoes, from figures in Vogt (1974) and Francis and Abbott (1973): frequency distributions for oceanic and continental volcanoes.

Height, km (lower class limit)	*0*	*1*	*2*	*3*	*4*	*5*	*6*	*7*
oceanic (adjusted)	1	5	16	12	9	7	4	2
continental conical	35	85	42	17	1	1		

(1 to 7.5 km, corrected for buoyancy of submerged bases of the volcanoes: Table 2) increased with the square root of age of the basement crust. For a given basement age, there is only a two-fold range in volcano height. Relative height is thus limited by lithospheric thickness and temperature, but support from seawater permits oceanic volcanoes such as Hawaii to reach greater heights than continental ones.

Pike (1978) recognised 20 classes in a population of 655 terrestrial volcanic edifices and gave geometric means of their dimensions. Ranges of one standard deviation above and below the mean are around four-fold, implying logarithmic standard deviations a little greater than those for cirques given above (Table 1) but still consistent with scale-specificity. As in the case of landslides, classification (on criteria other than size) may be a prerequisite to recognition of scale-specificity.

Vogt (1974a) gave histograms for volcano spacing in various tectonic settings: spacing averages 40–100 km along subduction zones or hot-spot tracks and is approximately equal to lithosphere thickness. Median separations are 55 km in island arcs, 70 km in continental subduction zones. 'Hot spot' volcanoes in young lithosphere are 35 km apart for the New England seamounts, 42 km in Galapagos, and 52 km in the Azores. The Hawaii-Emperor chain lies on older (Cretaceous) crust and median spacing is 72 km, while on still older crust the Cape Verde, Canary and Cameroon volcanoes are 80 km apart. These differences support the importance of lithospheric age (and thus thickness) rather than plate velocity, in controlling volcano spacing. For eastern Africa Mohr and Wood (1976) confirmed the importance of lithospheric thickness, but disagreed with Vogt's hypothesis of fracture control. Spacings of 10 and 19 km in the very young crust of Erta-ali and Dubbi in Afar rise to 42 km along the Ethiopian and Gregory Rifts, 70–75 km in the Harar and eastern Uganda plateaux and Addis Ababa region, and 109 km on the Ethiopian Plateau (Oligocene and Miocene volcanoes). They also found that composition (basaltic, silicic or alkaline-carbonatitic) did not affect spacing. Both size and spacing of volcanoes are thus regionally scale-specific, and median spacing varies globally by one order of magnitude. Much greater spacing (over 500 km) on Mars suggests very thick lithosphere (Vogt, 1974a).

Where crust is rifting in the Red Sea, points of high heat flow about 50 km apart become the initial sites of oceanic crust formation (Bonatti, 1985). These 'asthenospheric diapirs' relate to instability in the upper mantle. Schouten *et al.* (1985, p. 225) found that "the volcanism that forms the oceanic crust along the

spreading-plate boundaries is concentrated at regular intervals related to spreading rate. ... the boundaries ... have a fairly rigorous cellular structure on a 30–80 km length scale." This seems to bear some relation to the volcano spacing discussed above. The spacing depends, however, on the one-third power of the magma production rate, and thus increases with Mid-Ocean Ridge spreading rate (Bonatti, 1985) to 140–180 km for the equatorial East Pacific Rise. A hierarchical series of overlapping along-ridge segment scales is recognised by Macdonald (1998): discontinuities between his third-order segments, 30 to 100 km long, correspond with breaks in magma chambers and are considered to be short-lived. His second-order discontinuities break Mid-Ocean Ridges into segments 50–230 km long that persist for several million years and are comparable to the cells discussed by Bonatti: they relate to overlapping spreading centres where magma supply is low.

Lava flows are also scale-specific. Walker (1973) demonstrated log-normal distributions of length for each chemical/viscosity group of flows. Median length is 4.1 km for basaltic and 1.3 km for acidic flows, but rate of effusion during the first few days is more important than viscosity as a control of length. Later work (in Chester, 1993, pp. 89–92) confirmed and extended Walker's conclusions. Pinkerton and Wilson (1994) developed a fuller model, and dealt with data sets showing a little over one order of magnitude variation in flow length. They confirmed Walker's conclusions, but demonstrated the effects of flow duration and gradient. Pelletier (1999), however, found a power-law distribution of areas of basaltic regions in western North America, between separation distances of 3 and 150 km: and of Hawaiian cinder cones, from 150 m to 7.5 km. He viewed the clustering of magmatism and volcanism as statistically self-similar in space and time.

Measuring the shape of lava flow outlines, Bruno *et al*. (1994) found fractal behaviour for basaltic flows on gentle slopes, but not for silicic flows. The latter showed convex fractal plots with clear scale breaks at 300 m or 2 km (in their figure 10 examples). This scale specificity is attributed to the higher viscosities and yield strengths, suppressing shortwave irregularity in silicic-flow outlines.

OCEAN FLOOR (TECTONIC AND VOLCANIC)

Young ocean floor on the flanks of Mid-Ocean Ridges shows transverse and strong longitudinal lineation, at regionally specific scales. Near-axis stretching of lithosphere produces lengthening normal faults perpendicular to spreading direction, giving multiple horsts and grabens. Perfit and Chadwick (1998) illustrated a number of Ridge flanks with kilometric-scale lineation. On the East Pacific Rise, Lonsdale (1977, p. 271 and figure 6) demonstrated "... marginal grabens spaced fairly regularly at 1.5 km intervals". He also illustrated (p. 255, figure 2) linear highs spaced c. 4 km apart.

Herzfeld *et al*. (1993) applied residual variograms to high-precision profiles 30 and 80 km long across two Pacific Mid-Ocean Ridges. Both showed clear scale dependence, with linear and Gaussian-linear geostatistical models applicable at different scales. Specific scales (ranges at which the increase of variance with separation levels out) of 6.75 and 10 km were found for the Juan de Fuca Ridge,

and 14 and 32 km for the faster-spreading East Pacific Rise. Herzfeld and Overbeck (1999) found apparent fractal dimensions around 2.3 for separations below 2 km, but around 2.54 from 2 to 10 km, results surprisingly similar to those for subaerial fluvial topography. The sea floor is smoother at local than at broader scales and is clearly anisotropic. Thus even though the spreading sea-floor of Mid-Ocean Ridges provides an environment where fewer processes are important than in sub-aerial topography, models of low dimensionality do not fit the complexity observed.

Carbotte and Macdonald (1994) found that fault scarp lengths and spacings in all their study areas followed exponential frequency distributions. For three areas in the Ecuador Rift and on the East Pacific Rise, characteristic lengths from the fitted exponential models were 5.8, 5.32 and 4.52 km; characteristic spacings were 1.21, 1.13 and 0.85 km. Mean lengths or spacings were rather greater in each case.

Fault scarp heights average 90 m: fault growth lasts for about 700 ka and often interacts with volcanism (Macdonald, 1998). This produces abyssal hills, covering over 30% of the ocean floor, and typically 50–300 m high, 2–5 km wide and 10–20 km long. Different models of interaction of faulting and volcanism apply to Mid-Ocean Ridges with different spreading rates and magma supplies. Detailed studies by ALVIN submersible on the fast-spreading, high-axis East Pacific Rise demonstrate that the abyssal hills there are essentially faulted volcanic structures, elongated parallel to Ridge axes (Macdonald *et al*., 1996). They develop asymmetrically as the outward-facing scarps are episodically draped by lava flows; these 'volcanic growth faults' are almost complete within 6 km of the Ridge axis. The inward-facing slopes are simpler fault scarps sloping 60–90° and continuing activity until over 30 km from the axis. Where spreading rates are low or magma in short supply, back-tilted fault blocks form the dominant abyssal hills. With more magma, intermediate spreading rates and a high axis, axial volcanoes are split as they move away from the axis, giving asymmetric abyssal hills even without tilting. Whole volcanoes are preserved mainly near axial discontinuities on fast-spreading Ridges (Macdonald *et al*., 1996).

Smith and Jordan (1987) proposed an exponential frequency distribution for large Pacific seamounts (submerged volcanoes). Wessel and Lyons (1997), however, preferred a power-law, assuming data inadequacy below 2 km height even in their improved satellite-geodesy-based data. They did show that many seamounts line up in 'hot-spot' chains, with height and density varying with age of oceanic crust: this suggests regional scale-specificity.

IMPACT CRATERS

Meteorite impact craters cover a broad range of scales, but when dimensions are plotted against each other there are breaks where power-law relations change. In fact, this may be the clearest example of scale-specificity bounding two scaling regimes. On the Moon, Pike (1967) observed a threshold depth of 2 km (diameter 15 km) beyond which rim-floor relative relief diminishes and central peaks appear. Rugged arcuate structural and slump terraces are found where crater

diameter exceeds 20 to 25 km. Further work established eleven changes in shape between diameters of 10 and 30 km, averaging 18.7 km on the Moon. Work on Mars found similar morphological transitions, but at a diameter of about 5 km (Pike, 1980, 1988): on Earth it averages 3 km and on Mercury 16 km (later revised to 10 km: Pike, 1988). Ejecta on Mars show signs of flow for craters 4 to 60 km in diameter: this probably comes from incorporation of subsurface volatiles (water, carbon dioxide). The huge energy involved in producing craters over 80 km in diameter probably evaporates the volatiles, or masks their flow effects.

The depth: diameter break in slope (intersection of lines fitted to simple and to complex craters) was refined to 1.9 km on Earth, 3.1 on Mars, 10 on Mercury (later revised to 4.7 km) and 10.9 km for the Moon (Pike, 1980, 1988, table XI). Figure 4 shows log-log scaling plots for Mars, the Moon and a comparison of planets. The transition is at smaller diameters in sedimentary rocks and in the layered lavas of lunar maria and Martian plains. Thus the transition size is negatively related to gravity and to rock layering and weakness. Clearly we are dealing here with a major process threshold. The fact that central peaks appear in smaller craters than do rimwall terraces was used by Pike (1980) to argue against centripetal slumping and deep sliding as the initiating process: deformation is shallow and in large complex craters inertially-driven central rebound occurs during impact, generating the inward displacement and rimwall failure.

Studies of large features established a further transition, to basins with concentric multiple rings. Pike (1985, 1988) observed a 'root-two times diameter' scaling of ring spacing for multi-ring basins on all planets and moons examined. In that a given wavelength dominates a region, this is a regional scale-specificity even though many wavelengths (above a threshold) are globally possible. Pike (1988, figure 10) provided fuller information on the simple to complex crater transition, and recognised a progression with size from simple through modified-simple and immature-complex to complex craters, then protobasins, two-ring basins and multiring basins. He also updated comparisons between planets (and moons).

Recently Schenk (2002) has made further use of these relationships, on three of Jupiter's moons. The transition from simple to complex occurs at 250 m on Ganymede, and 300 m on both Callisto and Europa. The next transition, to ringed structures, comes at 26 km on the first two, but at 8 km on Europa. Finally, Ganymede and Callisto show a further transition (at 60 km on older craters, 150 km in younger) to anomalous domes with poor rims; this is found at 30 km on Europa, but has not been found elsewhere. Schenk's interpretation is that warmer ice at depth is weaker than brittle, very cold ice near the surface. At greater depth, this warm ice completely covers an 'ocean'. Schenk infers that the warm ice is at 16 to 22 km depth on the first two moons and the ocean is over 80 km down: the figures for Europa are 7–8 km and 19–25 km respectively. Hence it is possible to constrain models of structure by establishing specific scales in morphology.

Like other artificial landforms, artificial craters produced in a given period are much more scale-specific in size. Westing and Pfeiffer (1972) estimated that 26 million craters were produced in Indochina from 1965 to 1971, mainly in South

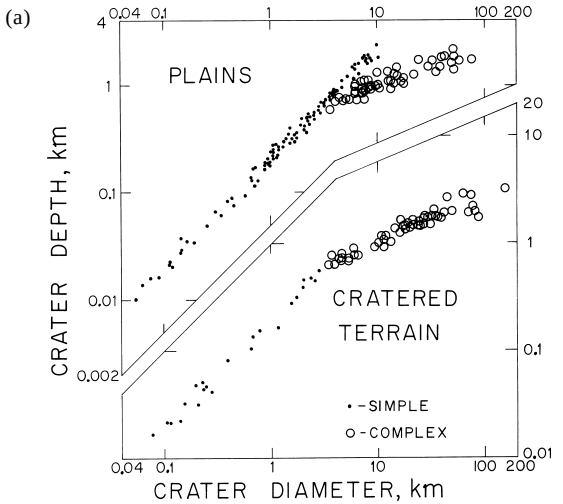

Fig. 4. Breaks in the crater depth: diameter scaling relation, illustrating the morphologic transition from simple to complex craters, from Pike (1980, figures 6, 9 and 2). (a) 230 craters on Mars, showing larger simple craters on plains than on 'cratered terrain'. (b) Based on 203 mare craters and 136 upland craters on the Moon. Simple craters follow a similar relation for maria and for uplands (as for the two divisions of Mars), but complex craters average 12% deeper in uplands. (c) Summary of the relationships on three planets and the Moon. The transition size increases as gravity decreases.

Vietnam. Most were from 500-pound bombs, and the craters were 1.5 to 6 m deep and 6 to 12 m in diameter.

DISCUSSION AND CONCLUSION

"... we ignore scale-dependency at our peril" (Wood, 1999). Iwahashi *et al*. (2001, p. 853) agree that "Geomorphic phenomena are scale-dependent, commonly irregular—even random—at high resolution, but exhibiting order at coarser scales." Frequent references by geomorphologists to typical landform sizes and various types of spatial regularity imply that the land surface is not scale-free (self-affine). If all landforms scale over broad ranges, why do we so often mention size in our initial description of a landform type? My literature search for hard evidence of size distributions has often been disappointing in that consistent measurements of large sets of landforms, producing frequency distributions, are much less common than vague assertions about size or spacing. Some evidence from different authors is conflicting, authors rarely compare power, exponential and log-normal models of frequency distributions, and the existence of a declining frequency of smaller forms needs careful testing when distributions are skewed. Progressive omission of smaller features is always a question, but does not explain the bimodality found in some dune size-frequency distributions. Our understanding of many landform types is incomplete: we need many more

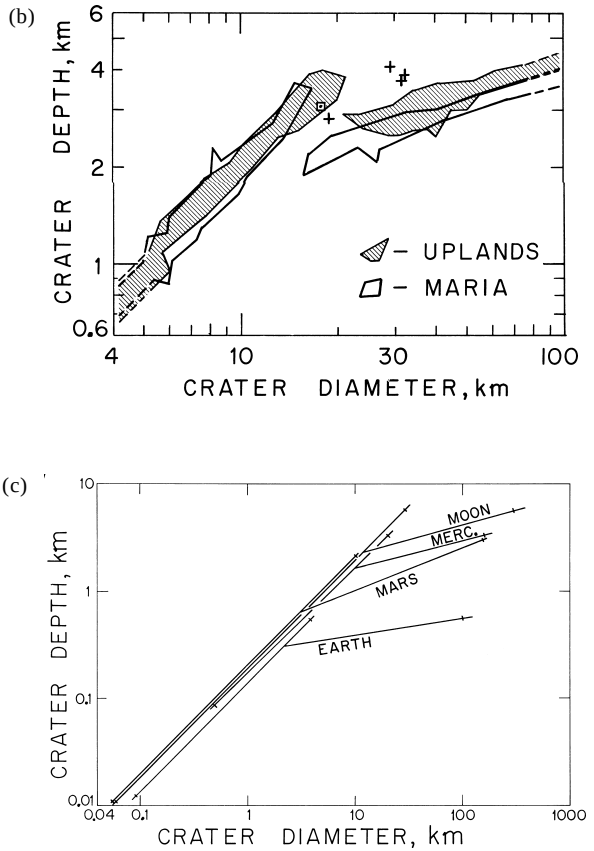

Fig. 4. (continued).

comprehensive frequency distributions of landform size and spacing to distinguish the very different models proposed and to establish the extent of scale-specificity (as manifest in log-normal or exponential distributions)—global, regional or local.

Scale-specificity has nevertheless been demonstrated for the size and spacing of specific landforms in aeolian, glacial, karst, tectonic, volcanic and meteoritic geomorphology, and for certain aspects of fluvial and slope geomorphology. It is found on a range of planets and moons. Juxtaposition of results from diverse branches of geomorphology has been valuable in demonstrating the scope for cross-fertilization in concepts and methods. I do not have space here to discuss the excellent examples of scale-specificity in coastal and periglacial geomorphology, or in patterned ground or microrelief. The pingos of permafrost areas are scale-specific. There are of course very clear examples of local scale-specificity in channel forms such as meanders, bars and pool-riffle sequences.

Further scales, etched into topography by erosion, are inherited from structural features such as jointing, faulting and bedding.

Only a mention can be made of the importance attached to scale considerations in (largely fluvial) process studies (e.g. Church, 1996), relevant though that is to development of scaled bedforms. However, the concept of 'Representative Elementary Area', "a fundamental scale for catchment modelling at which continuum assumptions can be applied" (Wood *et al.*, 1990) appears to be an explicit recognition of scale specificity. Dietrich and Montgomery (1998) and Beven (1995) discussed the importance of including realistic scale effects in landscape modelling and hydrological modelling respectively. Process modellers are forced to take scale into account both by the reality of specific scales in the land surface (as discussed here) and by practical data and modelling considerations.

Scale specificity of landforms is common in both the land surface and the sea floor, and arises in several different ways. Each specific scale raises questions of the processes or constraints responsible: some scales in different thematic fields (process systems) are interrelated. For example, cirques and landslides are constrained spatially by the dimensions of the slopes or valleys in which they develop. Processes exhibit thresholds of depth, width or velocity, or sizes of circulation cells, which may relate to scale-specific landforms (especially bedforms). Whether the specificity is global, regional or local, it is a clear feature of the land surface and a deviation from general mathematical models of the surface. Yet our precise knowledge of size and spacing is surprisingly limited: geomorphologists have become more sensitive to issues of temporal scale, but they should not lose sight of related issues of spatial scale (Phillips, 1988).

Scale dependence involves scaling (either isometric or allometric), scale breaks (thresholds) and scale-specific frequency distributions. Both the establishment of scaling relationships over certain ranges, and the recognition of scale-specific features and processes, are among the important tasks of geomorphology. The concept of 'scaling' remains valuable if the range of scales over which it applies is clearly specified: commonly this is between one and three decimal orders of linear magnitude. As Mark and Aronson (1984, p. 681) put it, for their study of variograms for Appalachian and western USA regions, "In a certain sense ... both conventional geomorphic wisdom ('landscapes have characteristic scales') and the fractals model ('geomorphic surfaces are statistically self-similar') are 'correct' ".

The existence of thresholds, breaks in slope and other limits means that, in earth sciences, scaling never applies over unlimited ranges: it is thus foolish to extrapolate. This rules out the use of scaling relationships to make up for limited measurement resolution or to 'extend the range' of data: their use should be confined to interpolation and estimation within the range of the data. Where characteristic scales can be established, they provide important clues to process and basic concepts for a discipline, parts of its broader framework and connective tissue. I assert that most recognisable landform types are scale-specific, at least regionally or locally.

Acknowledgements—Based on a presentation to 5th International Geomorphological Conference, Tokyo August 2001, S19: New concepts and modelling in geomorphology. Comments by Nick Cox, David Higgitt and Richard Pike have led to significant improvements. Hiroo Ohmori and Toshihiko Sugai kindly provided their landslide data file. Figure 4(a)–(c) is reproduced with kind permission of Richard Pike. This review is dedicated to the memory of Richard J. Chorley (1927–2002), who turned British geomorphology from an introspective art into an outward-looking science.

REFERENCES

Allen, J. R. L. (1982) Sedimentary structures: their character and physical basis: *Developments in Sedimentology*, **30**, 2 vols., Elsevier, Amsterdam, 593 + 663 pp.

Bechtel, T. D., Forsyth, D. W., Sharpton, V. L. and Grieve, R. A. F. (1990) Variations in effective elastic thickness of the North American lithosphere: *Nature*, **343**, 636–638.

Beven, K. (1995) Linking parameters across scales: subgrid parameterisations and scale dependent hydrological modelling: In J. D. Kalma and M. Sivapalan (eds.), *Scale Issues in Hydrological Modelling*, pp. 263–282. J. Wiley, New York.

Bird, P. (1991) Lateral extrusion of lower crust from under high topography, in the isostatic limit: *J. Geophys. Res.*, **96**, 10275–10286.

Blair, R. W. (1994) Moraine and valley-wall collapse due to rapid deglaciation in Mount Cook National Park, N.Z.: *Mountain Research and Development*, **14**, 347–358.

Blair, T. C. and McPherson, J. G. (1994) Alluvial fan processes and forms: In A. D. Abrahams and A. Parsons (eds.), *Geomorphology of Desert Environments*, pp. 354–402. Chapman & Hall, London.

Bonatti, E. (1985) Punctiform initiation of sea-floor spreading in the Red Sea during transition from a continental to an oceanic rift: *Nature*, **316**, 33–37.

Brozovic, N., Burbank, D. W. and Meigs, A. J. (1997) Climatic limits on landscape development in the Northwestern Himalaya: *Science*, **276**, 571–574.

Bruno, B. C., Taylor, G. J., Rowland, S. K. and Baloga, S. M. (1994) Quantifying the effect of rheology on lava-flow margins using fractal geometry: *Bulletin of Volcanology*, **56**, 193–206.

Burbank, D. W., Leland, J., Fielding, E., Anderson, R. S., Brozovic, N., Reid, M. R. and Duncan, C. (1996) Bedrock incision, rock uplift and threshold hillslopes in the northwestern Himalayas: *Nature*, **379**, 505–510.

Carbotte, S. M. and Macdonald, K. C. (1994) Comparison of seafloor tectonic fabric at intermediate, fast and superfast spreading ridges: influence of spreading rate, plate motions, and ridge segmentation on fault patterns: *J. Geophys. Res.*, **99**(B7), 13,609–13,631.

Chester, D. (1993) *Volcanoes and Society*. Edward Arnold, London, 351 pp.

Church, M. (1996) Space, time and the mountain—how do we order what we see?: In B. L. Rhoads and C. E. Thorn (eds.), *The Scientific Nature of Geomorphology: Proc. 27th Binghamton Symposium in Geomorphology*. J. Wiley, New York.

Church, M. and Mark, D. M. (1980) On size and scale in geomorphology: *Progress in Physical Geography*, **4**(3), 342–390.

Cooke, R. U., Warren, A. and Goudie, A. S. (1993) *Desert Geomorphology*. UCL Press, London, 526 pp.

Cox, N. J. (1992) Precipitation statistics for geomorphologists: variations on a theme by Frank Ahnert: *Catena*, Supplement, **23**, 189–212.

Day, M. J. (1978) Morphology and distribution of residual limestone hills (mogotes) in the karst area of northern Puerto Rico: *Geol. Soc. Am. Bull.*, **89**, 426–432.

De Blasio, F. V. (2002) Note on simulating the size distribution of glacial cirques: *Earth Surf. Processes Landf.*, **27**, 109–114.

de Silva, S. L. and Francis, P. W. (1991) *Volcanoes of the Central Andes*. Springer, Berlin.

Dietrich, W. E. and Montgomery, D. R. (1998) Hillslopes, channels and landscape scale: In G. Sposito (ed.), *Scale Dependence and Scale Invariance in Hydrology*, pp. 30–60. Cambridge U.P.

Dietrich, W. E., Wilson, C. J., Montgomery, D. R. and McKean, J. (1993) Analysis of erosion thresholds, channel networks, and landscape morphology using a Digital Terrain Model: *Journal of Geology*, **101**, 259–278.

Evans, I. S. (1972) General geomorphometry, derivatives of altitude, and descriptive statistics: Ch. 2 In R. J. Chorley (ed.), *Spatial Analysis in Geomorphology*, pp. 17–90. Methuen, London.

Evans, I. S. (1997) Process and form in the erosion of glaciated mountains: Ch. 7 In D. R. Stoddart (ed.), *Process and Form in Geomorphology*, pp. 145–174. Routledge, London.

Evans, I. S. and McClean, C. J. (1995) The land surface is not unifractal; variograms, cirque scale and allometry: *Zeitschrift für Geomorphologie*, N.F. Supplement-Band, **101**, 127–147.

Francis, P. W. and Abbott, B. M. (1973) Sizes of conical volcanoes: *Nature*, **244**, 22–23.

Goldie, H. S. and Cox, N. J. (2000) Comparative morphometry of limestone pavements in Switzerland, Britain and Ireland: *Zeitschrift für Geomorphologie*, N.F. Supplement-Band, **122**, 85–112.

Gordon, J. E., Whalley, W. B., Gellatly, A. F. and Vere, D. M. (1992) The formation of glacial flutes: assessment of models with evidence from Lyngsdalen, North Norway: *Quaternary Science Reviews*, **11**, 709–731.

Goudie, A. S. (1999) Wind erosional landforms: yardangs and pans: In A. S. Goudie, I. Livingstone and S. Stokes (eds.), *Aeolian Environments, Sediments and Landforms*, pp. 167–180. J. Wiley, Chichester.

Gravenor, C. P. and Meneley, W. A. (1958) Glacial flutings in central and northern Alberta: *American Journal of Science*, **256**, 715–728.

Greeley, R. and Iversen, J. D. (1985) Wind as a geological process; on Earth: *Mars, Venus and Titan*. Cambridge U.P., 333 pp.

Hagedorn, H. (1971) Untersuchungen über Relieftypen arider Räume an Beispielen aus dem Tibesti-Gebirge und seiner Umgebung: *Zeitschrift für Geomorphologie*, N.F. Supplement-Band, **11**, 251 pp.

Hallet, B., Hunter, L. and Bogen, J. (1996) Rates of erosion and sediment evacuation by glaciers: a review of field data and their implications: *Global & Planetary Change*, **12**, 213–235.

Herzfeld, U. C., Kim, I. I., Orcutt, J. A. and Fox, C. G. (1993) Fractal geometry and sea-floor topography: theoretical concepts versus data analysis for the Juan de Fuca Ridge and the East Pacific Rise: *Annales Geophysicae*, **11**(6), 531–541.

Herzfeld, U. C. and Overbeck, C. (1999) Analysis and simulation of scale-dependent fractal surfaces with applications to seafloor morphology: *Computers and Geosciences*, **25**, 979–1007.

Hovius, N. (1996) Regular spacing of drainage outlets from linear mountain belts: *Basin Research*, **8**, 29–44.

Hovius, N. (2000) Macroscale process systems of mountain belt erosion: In M. A. Summerfield (ed.), *Geomorphology and Global Tectonics*, pp. 77–105. J. Wiley, New York.

Iwahashi, J., Watanabe, S. and Furuya, T. (2001) Landform analysis of slope movements using DEM in Higashikubiki area, Japan: *Computers & Geosciences*, **27**, 851–865.

Johnson, N. L., Kotz, S. and Balakrishnan, N. (1994) *Continuous Univariate Distributions*, Vol. 1, 2nd ed., J. Wiley, New York, 719 pp.

Klimchouk, A. and Andrejchuk, V. (1996) Breakdown development in cover beds, and landscape features induced by intrastratal gypsum karst: *Int. Jour. Speleology*, **25**(3–4), 127–144.

Lancaster, N. (1988) Controls of eolian dune size and spacing: *Geology*, **16**, 972–975.

Lancaster, N. (1989) Star dunes: *Progress in Physical Geography*, **13**, 67–91.

Lonsdale, P. (1977) Structural geomorphology of a fast-spreading rise crest—the East Pacific Rise near 3.25 S.: *Marine Geophys. Res.*, **3**, 251–293.

Macdonald, K. C. (1998) Linkages between faulting, volcanism, hydrothermal activity and segmentation on fast spreading centres: In W. R. Buck, P. T. Delaney, J. A. Karson and Y. Lagabrielle (eds.), *Faulting and Magmatism at Mid-Ocean Ridges*, pp. 27–58. American Geophysical Union, Washington, D.C.

Macdonald, K. C., Fox, P. J., Alexander, R. T., Pockalny, R. and Gente, P. (1996) Volcanic growth faults and the origin of Pacific abyssal hills: *Nature*, **380**(6570), 125–129.

Mainguet, M. (1972) *Le modelé des grès: problèmes généraux*. Institut Géographique National, Paris.

McClean, C. J. and Evans, I. S. (2000) Apparent fractal dimensions from continental scale digital elevation models using variogram methods: *Transactions in GIS*, **4**(4), 361–378.

Mark, D. M. and Aronson, P. B. (1984) Scale-dependent fractal dimensions of topographic surfaces: an empirical investigation, with applications in geomorphology and computer mapping: *Mathematical Geology*, **16**(7), 671–683.

Mills, H. H. (1987) Morphometry of drumlins in the northeastern and north-central USA.: In J. Menzies and J. Rose (eds.), *Drumlin Symposium*, pp. 131–147. A. A. Balkema, Rotterdam.

Mohr, P. A. and Wood, C. A. (1976) Volcano spacings and lithospheric attenuation in the Eastern Rift of Africa: *Earth & Planetary Science Letters*, **33**, 126–144.

Montgomery, D. R. and Dietrich, W. E. (1992) Channel initiation and the problem of landscape scale: *Science*, **255**, 826–830.

Montgomery, D. R., Sullivan, K. and Greenberg, H. M. (1998) Regional test of a model for shallow landsliding: *Hydrological Processes*, **12**, 943–955.

Mottershead, D. (1996) A study of flutes (Rillenkarren) at Lluc, Majorca: *Zeitschrift für Geomorphologie*, N.F. Supplement-Band, **103**, 215–241.

Oguchi, T. (1997) Drainage density and relative relief in humid steep mountains with frequent slope failure: *Earth Surf. Processes Landf.*, **22**, 107–120.

Ohmori, H. and Sugai, T. (1995) Toward geomorphometric models for estimating landslide dynamics and forecasting landslide occurrence in Japanese mountains: *Zeitschrift für Geomorphologie*, N.F. Supplement-Band, **101**, 149–164.

Pelletier, J. D. (1999) Statistical self-similarity of magmatism and volcanism: *J. Geophys. Res.* **104**(B7), 15,425–15,438.

Perfit, M. R. and Chadwick, W. W. (1998) Magmatism at Mid-Ocean Ridges: constraints from volcanological and geochemical investigations: In W. R. Buck, P. T. Delaney, J. A. Karson and Y. Lagabrielle (eds.), *Faulting and Magmatism at Mid-Ocean Ridges*, pp. 59–115. American Geophysical Union, Washington, D.C.

Phillips, J. D. (1988) The role of spatial scale in geomorphic systems: *Geographical Analysis*, **20**(4), 308–317.

Pike, R. J. (1967) Schroeter's Rule and the modification of lunar crater impact morphology: *J. Geophys. Res.*, **72**(8), 2099–2106.

Pike, R. J. (1978) Volcanoes on the inner planets: some preliminary comparisons of gross topography: *Proceedings, Lunar & Planetary Science Conference, 9th*, 3239–3273.

Pike, R. J. (1980) Control of crater morphology by gravity and target type: Mars, Earth, Moon: *Proceedings, Lunar & Planetary Science Conference, 11th*, 2159–2189.

Pike, R. J. (1985) Some morphological systematics of complex impact structures: *Meteoritics*, **20**(1), 49–68.

Pike, R. J. (1988) Geomorphology of impact craters on Mercury: In F. Vilas, C. R. Chapman and M. S. Matthews (eds.), *Mercury*, pp. 165–273. Univ. of Arizona Press, Tucson AZ.

Pike, R. J., Acevedo, W. and Card, D. H. (1989) Topographic grain automated from digital elevation models: *Proceedings, Auto-Carto 9, ASPRS/ACSM Baltimore MD, 2–7 April 1989*, 128–137.

Pinkerton, H. and Wilson, L. (1994) Factors controlling the lengths of channel-fed lava flows: *Bulletin of Volcanology*, **56**, 108–120.

Sauerman, G., Rognon, P., Poliakov, A. and Herrmann, H. J. (2000) The shape of the barchan dunes of southern Morocco: *Geomorphology*, **36**, 47–62.

Schenk, P. M. (2002) Thickness constraints on the icy shells of the Galilean satellites from a comparison of crater shapes: *Nature*, **417**(6887), 419–421.

Schmidt, K. M. and Montgomery, D. R. (1995) Limits to relief: *Science*, **270**, 617–620.

Schouten, H., Klitgord, K. D. and Whitehead, J. A. (1985) Segmentation of Mid-Ocean Ridges: *Nature*, **317**(6034), 225–229.

Smith, D. K. and Jordan, T. H. (1987) The size distribution of Pacific seamounts: *Geophys. Res. Letters*, **14**, 1119–1122.

Stark, C. P. and Hovius, N. (2001) The characterization of landslide size distributions: *Geophys. Res. Letters*, **28**, 1091–1094.

Sugai, T., Ohmori, H. and Hirano, M. (1994) Rock control on magnitude-frequency distribution of landslide: *Trans., Japan Geomorph. Union*, **15**, 233–251.

Tarboton, D. G., Bras, R. L. and Rodriguez-Iturbe, I. (1992) A physical basis for drainage density: *Geomorphology*, **5**, 59–76.

Troester, J. W., White, E. L. and White, W. B. (1984) A comparison of sinkhole depth frequency distributions in temperate and tropic karst regions: In B. F. Beck (ed.), *Sinkholes: Their Geology, Engineering and Environmental Impact*, pp. 65–73. A. A. Balkema, Rotterdam.

Vandekerckhove, L., Poesen, J., Oostwoud Wijdenes, D., Nachtergaele, J., Kosmas, C., Roxo, M. J. and de Figueiredo (2000) Thresholds for gully initiation and sedimentation in Mediterranean Europe: *Earth Surf. Processes Landf.*, **25**(11), 1201–1220.

Vergne, M. and Souriau, M. (1994) A multi-scale analysis of continental relief in southern France: *Int. Jour. Remote Sensing*, **15**(2), 2409–2419.

Vogt, P. R. (1974a) Volcano spacing, fractures, and thickness of the lithosphere: *Earth & Planetary Science Letters*, **21**, 235–252.

Vogt, P. R. (1974b) Volcano height and plate thickness: *Earth & Planetary Science Letters*, **23**, 337–348.

Walker, G. P. L. (1973) Lengths of lava flows: *Philosophical Trans., Royal Soc. London*, **A274**, 107–118.

Wasson, R. J. and Hyde, R. (1983a) Factors determining desert dune type: *Nature*, **B304**, 337–339 [Discussion (1984) *Nature*, **309**, 91–92].

Wasson, R. J. and Hyde, R. (1983b) A test of the granulometric control of desert dune geometry: *Earth Surf. Processes Landf.*, **8**, 301–312.

Wasson, R. J., Fitchett, K., Mackey, B. and Hyde, R. (1988) Large-scale patterns of dune type, spacing and orientation in the Australian continental dunefield: *Australian Geographer*, **19**, 89–104.

Wessel, P. and Lyons, S. (1997) Distribution of large Pacific seamounts from Geosat/ERS-1: implications for the history of intraplate volcanism: *J. Geophys. Res.*, **102**(B10), 22,459–22,475.

Westing, A. H. and Pfeiffer, E. W. (1972) The cratering of Indochina: *Scientific American*, **226**(5), 20–29.

White, W. B. and White, E. L. (1987) Ordered and stochastic arrangements within regional sinkhole populations: In B. F. Beck and W. L. Wilson (eds.), *Karst Hydrology: Engineering and Environmental Applications*, pp. 85–90. A. A. Balkema, Rotterdam.

Whitney, M. (1983) Eolian features shaped by aerodynamic and vorticity processes: In M. E. Brookfield and T. S. Ahlbrandt (eds.), *Eolian Sediments and Processes, Developments in Sedimentology*, **38**, pp. 223–245. Elsevier, Amsterdam.

Wilson, I. G. (1971) Desert sandflow basins and a model for the development of ergs: *Geographical Journal*, **137**, 180–199.

Wilson, I. G. (1972) Aeolian bedforms—their development and origins: *Sedimentology*, **19**, 173–210.

Wilson, J. P. and Gallant, J. C. (eds.), (2000) *Terrain Analysis: Principles and Applications*. J. Wiley, New York, 479 pp.

Wood, E. F., Sivapalan, M. and Beven, K. (1990) Similarity and scale in catchment storm response: *Reviews of Geophysics*, **28**(1), 1–18.

Wood, J. (1996) Scale-based characterization of digital elevation models: Ch. 13 In D. Parker (ed.), *Innovations in GIS 3*. Taylor and Francis, London.

Wood, J. (1999) Visualisation of scale dependencies in surface models: *Paper Presented at the International Cartographic Association Annual Conference, Ottawa 1999*.